Journal of Applied Polymer Science

Microcrystalline cellulose as reactive reinforcing fillers for epoxidized soybean oil polymer composites

Ming He,[1] Jianjun Zhou,[1] Huan Zhang,[1] Zhenyang Luo,[1] Jianfeng Yao[2]
[1]College of Science, Nanjing Forestry University, Nanjing 210037, China
[2]College of Chemical Engineering, Nanjing Forestry University, Nanjing 210037, China
Correspondence to: J. Yao (E-mail: jfyao@njfu.edu.cn)

ABSTRACT: Microcrystalline cellulose (MCC) and its oxidized product dialdehyde cellulose (DAC) were introduced as the reinforcing filler in epoxidized soybean oil (ESO) thermosetting polymer. The composites comprising up to 25 wt % cellulose fillers were obtained via a solution casting. The reinforcing effects of the cellulose were evaluated by microstructure analysis, dynamic mechanical analysis, and tensile and thermal stability tests. The results showed that at the same filler concentration, DAC led to higher stretching strength, modulus, and break elongation than MCC. The 5 wt % DAC loading in ESO polymer exhibits the highest toughness and thermal stability due to the good dispersion and interfacial interaction between DAC and ESO polymer matrix. The increased storage modulus and glass transition temperature also indicate the cellulose fillers impart stiffness to the composites. © 2015 Wiley Periodicals, Inc. J. Appl. Polym. Sci. **2015**, *132*, 42488.

KEYWORDS: biomaterials; cellulose and other wood products; composites

Received 27 February 2015; accepted 11 May 2015
DOI: 10.1002/app.42488

INTRODUCTION

The replacement of petroleum-based products by natural biorenewable resources has been received intensive attention in recent years due to the price fluctuation of petrochemical feedstock and environment pollution. Vegetable oil, as the cheapest and most abundant biological feedstock, has been studied extensively for composite and coating materials, and offers a promising potential for high performance biomass derived materials.[1] According to a lifecycle comparison, vegetable oil-based feedstocks show 75% less total environmental impacts than petroleum-based feedstocks due to significant reductions in fossil fuel consumption, global warming, smog formation, and ecological toxicity.[2] There are many reports that modified vegetable oils have been used to synthesize segmented polyurethane,[3] thermoplastic polyurethanes,[4] poly(methyl methacrylate) multigraft copolymers,[5] novel thermosetting rubbers,[6–8] and "green" composites.[9,10]

Epoxidized soybean oil (ESO) is a kind of triglyceride made up of a complex multi-component mixture of functionalized oleic, linoleic, and linolenic acid methyl esters as well as saturated fatty acids (i.e. palmitic and stearic acids). ESO has been investigated as starting materials to prepare thermosetting materials owing to their high reactivity of epoxy rings and versatilities. For example, bio-based thermosetting materials can be produced by curing the ESO through thermal and UV approaches.[11,12] However, the mechanical and thermal properties of ESO thermosets, such as tensile strength, Young's modulus, break elongation, and thermal stability, are generally lower than those of petroleum-based thermosets, such as epoxy and unsaturated polyester.[13,14] It could be mainly ascribed to the low crosslink density and flexibility of the backbone structure in ESO. To compensate these defects, some strategies have been implemented to improve the properties of ESO thermosets: incorporation of clay,[15] modification with silane coupling agent,[16] and blending with epoxy.[17–21] In most of the literature results, the impact strength and fracture toughness of the thermosets were improved, but the break elongation and the tensile strength were still low in some extend.[18,19,22]

Cellulose is one of the most abundant and renewable biopolymers in nature and is produced from plants, trees, bacteria, and sessile sea creatures of tunicates. Microcrystalline cellulose (MCC) is the hydrolyzed cellulose consisting of a large amount of cellulose microcrystals together with amorphous areas. MCC is a very promising cellulosic reinforcement for polymers due to the advantages of being biodegradable, renewable, low density, low cost, little abrasion to equipment, and good mechanical properties.[23,24] Composites from matrices such as polyurethane,[25] poly(vinyl alcohol),[26] wood plastic composites,[27] nylon 6,[28] and rubber[29] by using microcrystalline cellulose as a reinforcing filler have been achieved.

Apart from MCC, other derivatives of cellulose, such as hydroxyethylcellulose, carboxymethyl cellulose, and methylcellulose,

© 2015 Wiley Periodicals, Inc.

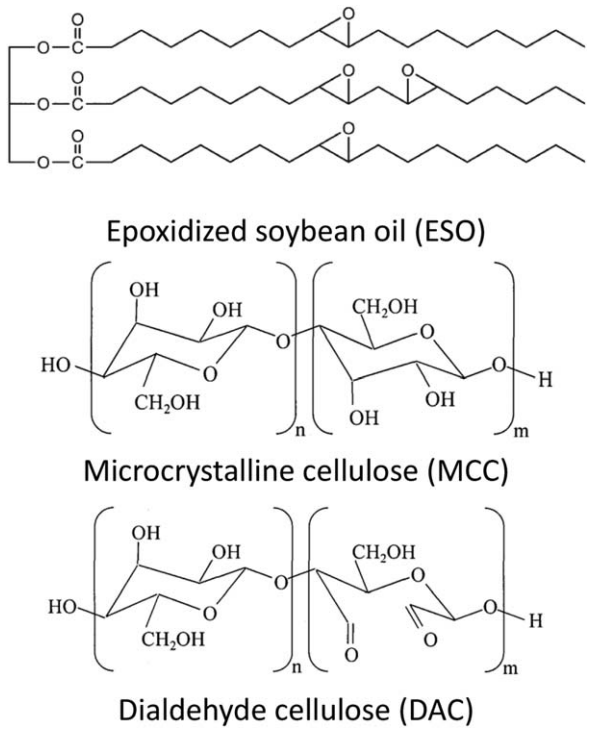

Figure 1. Chemical structure of the main reagents used in this study.

have been explored and widely used in the fields of foodstuff, pharmaceutical, and cosmetic industries by means of various modification methods. 2,3-Dialdehyde cellulose (DAC) is one kind of derivate produced by a regioselective oxidation of cellulose using periodate as an oxidation agent. Periodate is able to break the corresponding C–C bond between positions 2 and 3 of the glucopyranose ring of cellulose, simultaneously oxidizing vicinal hydroxyl groups.[30] Because the aldehyde groups of DAC have high reactivity towards further modification such as Schiff base reaction, cationization, and further oxidation to dicarboxylic acid and reduction to primary alcohols.[31,32] These changes favor the increase of accessibility and specific surface area of MCC with an improvement on reactivity. However, little work has been done on the effects of using DAC as the reinforcing filler in composites.

In this work, MCC and DAC were introduced as the reactive reinforcing fillers to the preparation of the MCC/ESO and DAC/ESO composites. The structural details of the composites were studied using scanning electron microscopy, and while the mechanical performance was examined using conventional tensile testing and dynamic mechanical thermal analysis.

EXPERIMENTAL

Materials

Epoxidized soybean oil (ESO, epoxy value: 0.375 mol/100 g) was received from Wuhu Aladdin Chemical Additives Co. (Wuhu, Anhui, China). The hardener cis-1,2-cyclohexanedicarboxylic anhydride (HHPA, >99%) and catalyst 1-Methylimidazole (1MI, >99%) were obtained from Aladdin industrial Corporation (Shanghai, China). Both HHPA and ESO were dried in vacuo overnight before use. MCC was purchased from Sinopharm Chemical Reagent Co. (Shanghai, China). Ethylene glycol, Sodium hydroxide (NaOH), and acetone were purchased from Nanjing Chemical Reagent Co. (Nanjing, China). Sodium periodate ($NaIO_4$) was purchased from Shanghai Shiyi Chemical Reagent Co. (Shanghai, China).

DAC was made from the laboratory by the literature reported.[31] MCC was oxidized to dialdehyde MCC in 0.06 mol L^{-1} $NaIO_4$ solution for 6 h under ambient condition and was preserved away from light. The final DAC products were obtained by washing with deionized water to remove the residual $NaIO_4$. Aldehyde content of DAC is determined to be 0.1048 mmol/g using the method reported in literature.[31] The chemical structures of ESO, MCC, and DAC are shown in Figure 1.

Preparation of Epoxidized Soybean Oil Polymer

The ESO polymer and the composites were both synthesized by a thermally cured method. Blending was performed in a one-stage process by the direct mixing of epoxy monomers with a stoichiometric amount of HHPA (1 : 0.75 molar ratio of epoxy/anhydride) and 3 wt % of catalyst 1MI (on the basis of the anhydride weight). MCC (or DAC) powder was dispersed in

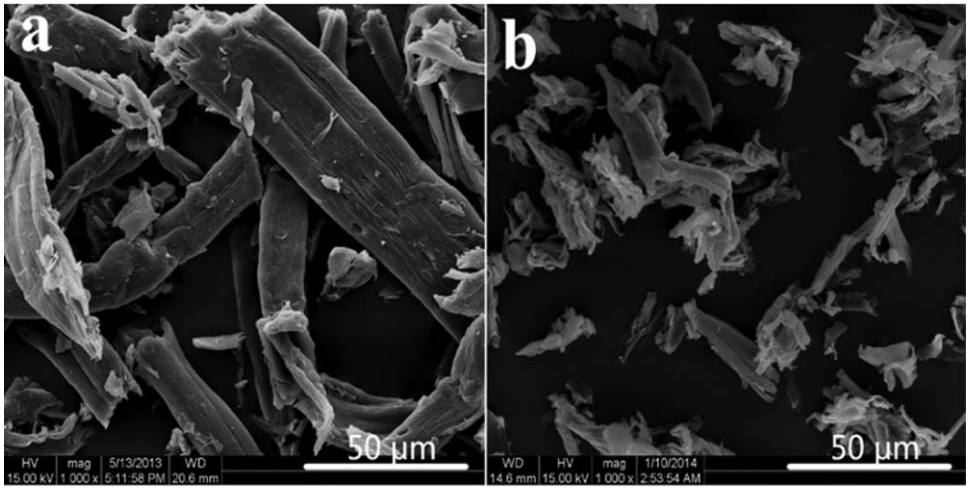

Figure 2. SEM images of (a) microcrystalline cellulose MCC and (b) dialdehyde cellulose DAC.

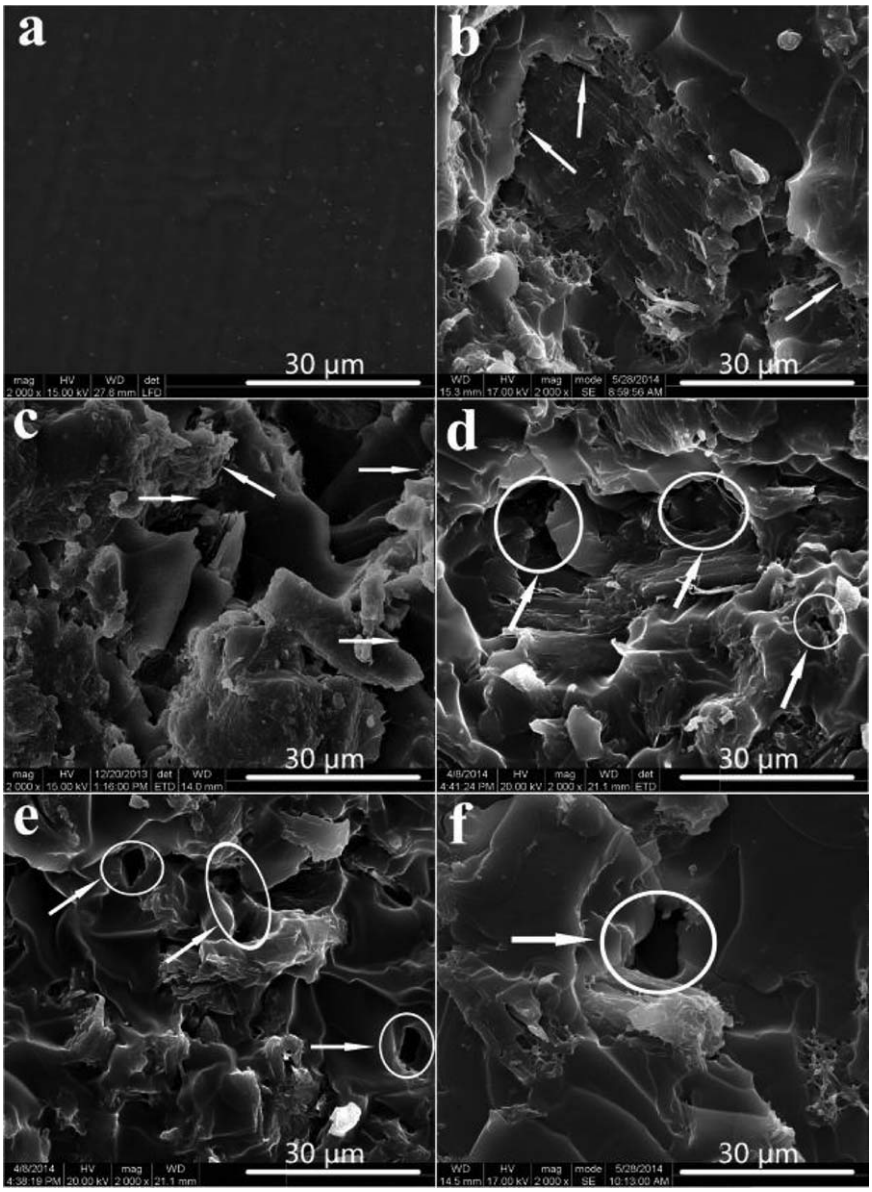

Figure 3. SEM images of fracture surfaces of the MCC/ESO composites with different MCC contents: (a) 0, (b) 5 wt %, (c) 10 wt %, (d) 15 wt %, (e) 20 wt %, and (f) 25 wt %.

acetone using an ultrasonic bath for 15 min. The content of additional cellulose was expressed as weight percentage of ESO (0, 5 wt %, 10 wt %, 15 wt %, and 20 wt %), respectively. All formulations were placed in a glass round-bottom flask and stirred at 60°C for 30 min. The mixing process was carried out under reduced pressure (~10 mmHg) to reduce the volume of air bubbles entrapped in the bulk. Subsequently, the reactive mixture was transferred into a polytetrafluoroethylene mold with a dimension of 125×115×10 mm^3. The mold had been previously heated to a temperature of 80~90°C in order to avoid thermal shock when the liquid resin was poured into the mold. The curing cycle chosen was heating for 1.5 h at 90°C, curing for 2 h at 100°C, and post-curing for 1 h at 110°C. From the cured sheets samples of different sizes were cut according to the different test standards.

Characterization

The morphology of fractured surfaces produced from the tensile samples was investigated by SEM (Quanta 200, FEI, USA). The samples were gold-coated to provide an electrically conductive surface. The accelerating voltage was lower than 20 kV to avoid excessive charge building up, which could cause the samples to degrade. Thermogravimetric analysis (TGA) was carried out under nitrogen atmosphere with a Thermogravimetric Analyzer (TG209F1, NETZSCH, Germany) at a heating rate of 10°C/min from 25 to 600°C.

The mechanical properties including the tensile strength (σ_b), elongation at break (ε_b), and Young's modulus (E) of the composite samples with a dimension of 75 ×6 ×1.5 mm^3 (length × width × thickness) were carried out at ambient condition on a universal testing machine (SUNS CMT5504, China) with a

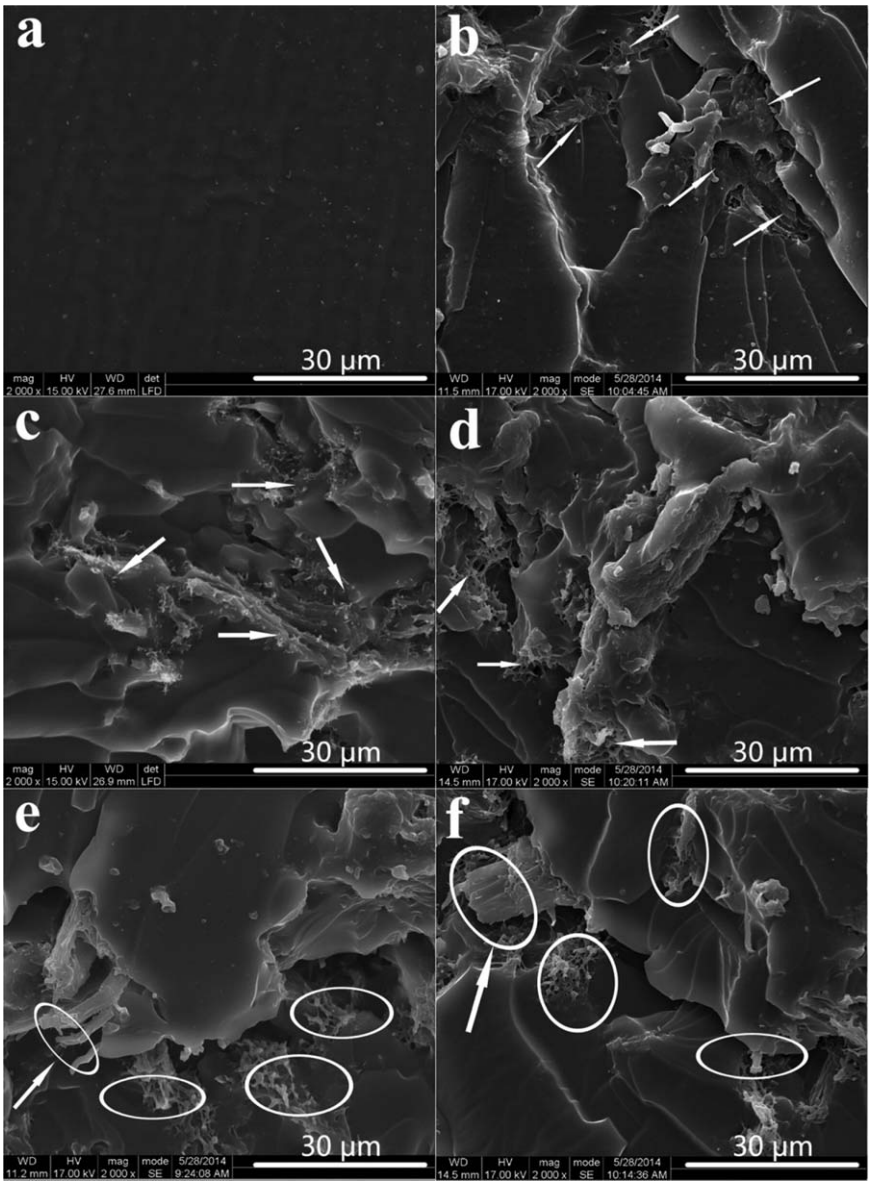

Figure 4. SEM images of fracture surfaces of the DAC/ESO composites with different DAC contents: (a) 0, (b) 5 wt %, (c) 10 wt %, (d) 15 wt %, (e) 20 wt %, and (f) 25 wt %.

loading rate of 100 mm min^{-1} at room temperature according to the standard of ISO 527-3:1996 (E). An average value of five replicates was taken. The dynamic properties of the neat ESO polymer and MCC (or DAC) reinforced composites were evaluated by a Dynamic Mechanical Analyzer (DMA 242 E, NETZSCH, Germany). Samples with a dimension of 35×5×1 mm^3 were tested in a single cantilever mode over a temperature range from −50 to 100°C, with a heating rate of 3°C/min at a frequency of 1 Hz to obtain storage modulus and tan delta.

RESULTS AND DISCUSSION

Morphology of the Composites

Figure 2 shows SEM images of MCC and DAC. It can be seen from the Figure 2(a) that the MCC particles are aggregates of crystalline cellulose with sizes of 20–150 μm. As the oxidant product of MCC, DAC shows a decreased fiber length and diameter, resulting in the aspect ratio change of the fibers [Figure 2(b)]. These characteristics of DAC are benefit to increase the specific surface area of cellulose and make better compatibility between cellulose and the matrix resin.

Figures 3 and 4 show the SEM images of the fractured surfaces of ESO polymer composites reinforced with MCC and DAC, respectively. From the fracture surfaces of Figure 3(a–f), the boundaries between the MCC fillers and ESO polymer matrix can be seen (indicated by the arrows), while the pure ESO matrix presents a smooth surface. With the increase of MCC content, the gaps between the fibers and the matrix, and the holes due to fiber pullout are observed (designated by a circle). These findings suggest that a weak interaction occurs between the matrix and MCC fillers.

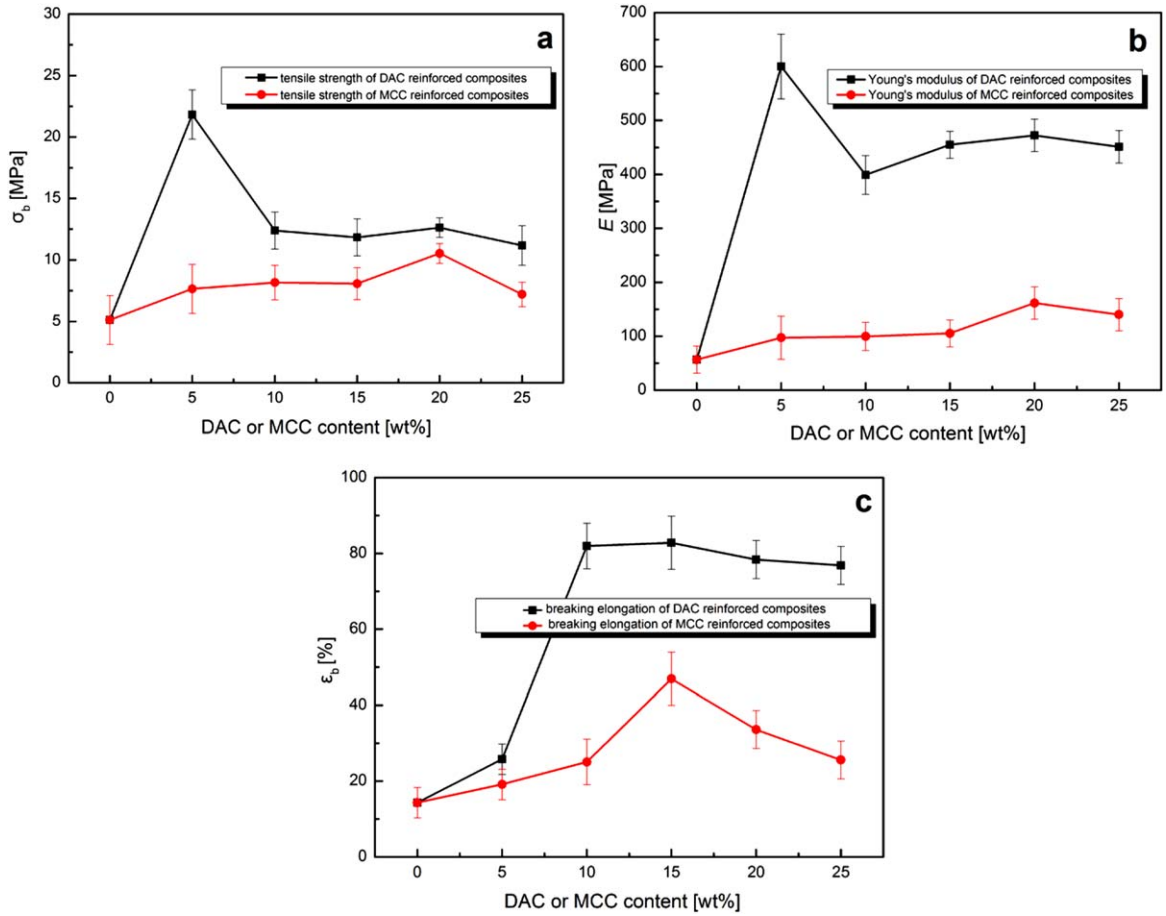

Figure 5. Effects of MCC or DAC content in the composites on tensile strength σ_b, Young's modulus E, and elongation at break ε_b. [Color figure can be viewed in the online issue, which is available at wileyonlinelibrary.com.]

In contrast, obvious difference can be found in DAC reinforced composites that the fractured surfaces show a more homogeneous and smoother surface with very small voids and few cavities [Figure 4]. This is an indication that a relatively stronger interfacial interaction occurs between DAC and the matrix. Particularly, when the DAC content is at 5 wt %, only a small amount of DAC fillers and minor cracks can be seen on the fractured surfaces (designated by the arrows in Figure 4(b)), indicating a reasonable level of miscibility between DAC and ESO polymer matrix. However when DAC content is over 20 wt %, more gaps and filler particles emerge, as shown in a circle in Figure 4(e,f). Meanwhile, some very fine fibrils on the fractured surfaces confirm the better dispersion of DAC fillers in the composites.

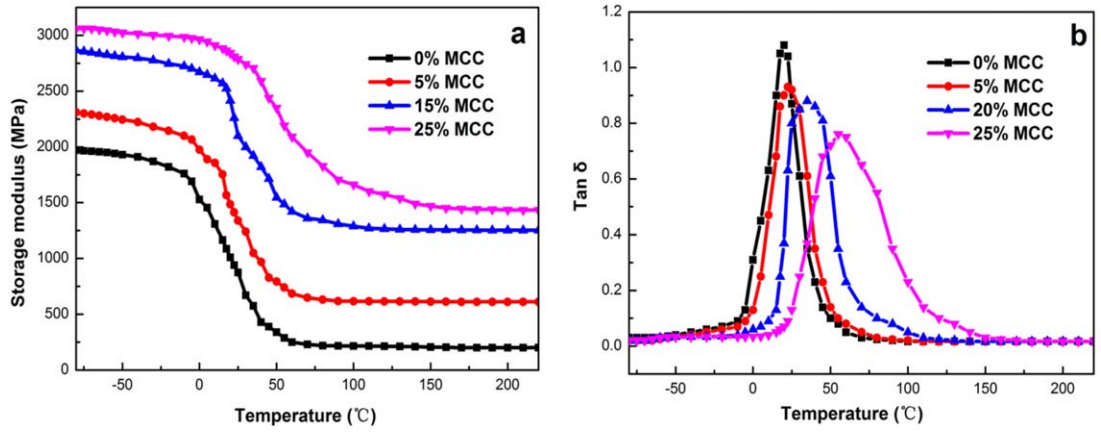

Figure 6. Storage moduli and tan δ of pure ESO polymer and MCC/ESO composites as a function of temperature. [Color figure can be viewed in the online issue, which is available at wileyonlinelibrary.com.]

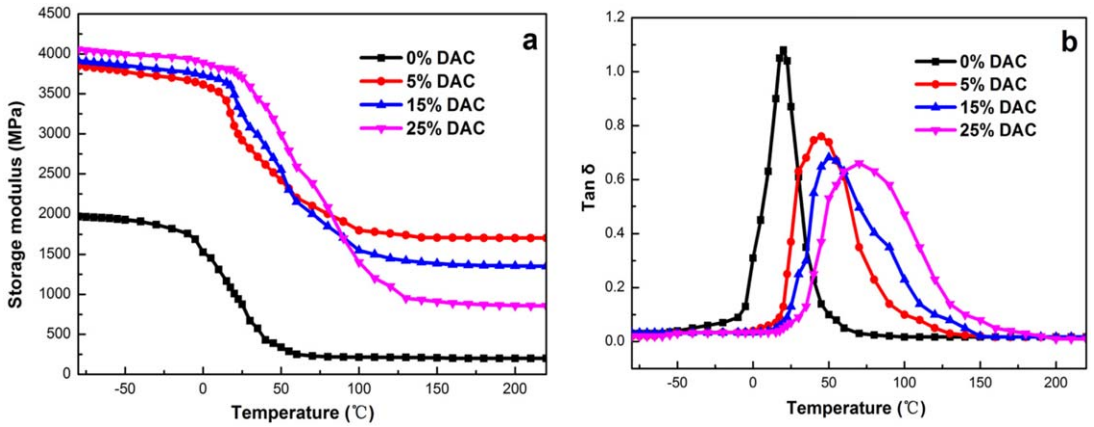

Figure 7. Storage moduli and tan δ of pure ESO polymer and DAC/ESO composites as a function of temperature. [Color figure can be viewed in the online issue, which is available at wileyonlinelibrary.com.]

Mechanical Properties of the Composites

Figure 5 shows the effects of different MCC and DAC contents on the mechanical properties of the MCC/ESO and DAC/ESO composites including tensile strength (σ_b), elongation at break (ε_b), and Young's modulus (E). These results exhibit a general trend: the properties increase and then decrease as both MCC and DAC contents increase, while DAC reinforced composites demonstrate better mechanical properties than MCC. This may be attributed to that DAC has a smaller dimension than MCC as well as the stronger interaction with the ESO polymer matrix. Furthermore, the composite comprising 5 wt % DAC shows the highest mechanical reinforcement, which may be due to the best dispersion of DAC in the ESO matrix as demonstrated by the SEM analysis [Figure 4(b)]. The decreases in mechanical properties at higher cellulose content are probably caused by cellulose agglomerations, where obvious interfaces and holes are presented [Figures 3 and 4].

It is also worth noting that the elongation at break is increased accompanying with the increase of tensile strength and Young's modulus. This toughening effect is caused by plastic

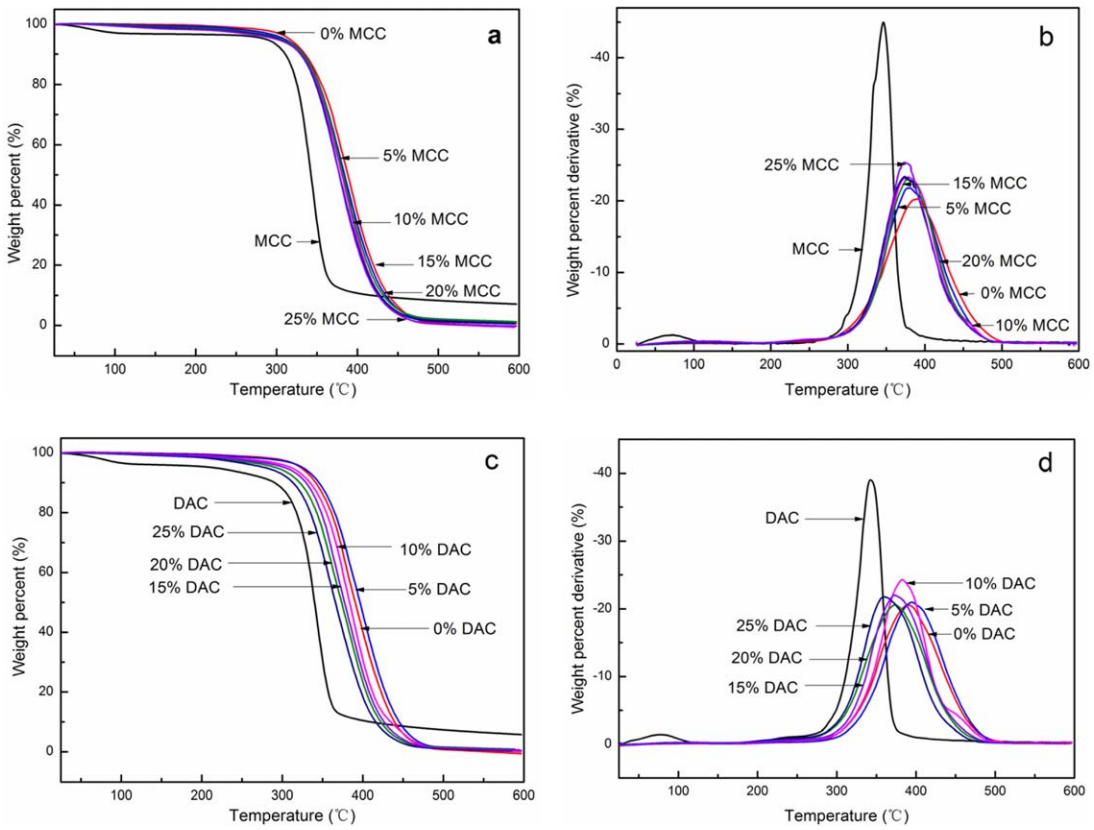

Figure 8. TG analyses and corresponding TGA curves of pure DAC, MCC, ESO polymer and MCC/ESO, DAC/ESO composites. [Color figure can be viewed in the online issue, which is available at wileyonlinelibrary.com.]

deformation of the matrix polymer induced by the interfacial debonding. Interfacial debonding releases strain constrains on the matrix polymer and lowers its plastic resistance, which allows plastic deformation to occur under suitable stress levels.[33] The maximum mechanical properties of MCC/ESO and DAC/ESO composites obtained at different filler contents can be explained by the interfacial bonding between cellulose and the matrix. This interfacial bonding is resulted from the hydroxyl groups and anhydride in the curing system.[34] With the significant decrease of particle size of cellulose by the oxidation reaction, more hydroxyl groups on the surface will interact with the matrix. Therefore, the maximum mechanical properties are obtained at a lower DAC content as compared to MCC.

Dynamic Mechanical Analysis

Dynamic mechanical analysis (DMA) allows determination of the mechanical behavior of materials over a broad temperature range and is strongly sensitive to the morphology and structure of the composites. Figures 6 and 7 show the storage modulus and tan δ of MCC/ESO and DAC/ESO composites, respectively, as a function of temperature. The storage modulus spectra show three district regions, which could be identified as glassy (temperature lower than -40°C), glass transition, and rubbery regions (higher than 50°C).

Compared to the pure ESO matrix, MCC/ESO composites show increased storage moduli over the entire temperature range, suggesting improved thermal-mechanical properties of the MCC/ESO composites with the increase of MCC content, indicating MCC fibers impart stiffness to the material. On the other hand, by incorporating MCC into the matrix, the glass transition temperature (Tg) of ESO polymer matrix shifts to a high temperature from 25°C to around 60°C. The increase of Tg is ascribed to the intermolecular interactions between the fillers and matrix, which reduces the flexibility of molecular chains of ESO matrix. A similar observation was reported for polylactic acid (PLA)/MCC composites.[35] Due to the better dispersion and the interaction with the matrix, the improvement in storage modulus of DAC/ESO composites is more remarkable, and the temperature of Tg shifts to a higher temperature of 70°C.

It can be noted that the ESO polymer matrix shows a narrow tan δ peak while the MCC/ESO (DAC/ESO) composites clearly show a broad tan δ peak [Figures 6(b) and 7(b)], which suggests that the relaxation processes slowly occur due to matrix-fibers interactions. Meanwhile, the intensity of tan δ peaks at Tg decreases with the addition of cellulose fillers, also indicating a constrained mobility of the polymeric matrix chains.

Thermogravimetric Analysis

TG analysis was conducted to investigate the thermal stability of pure MCC, DAC, ESO polymer, MCC/ESO, and DAC/ESO composites. The TG curves of the composites show only one thermal decomposition stage [Figure 8(a,c)], as confirmed in the corresponding TGA curves by the appearance of one maximum peak [Figure 8(b,d)], which is a proof of the good compatibility between the cellulose fillers and the ESO matrix. The decrease of the maximum degradation temperature with the increase of the filler loading could be explained by the lower thermal stability of the cellulose fillers compared to the pure ESO matrix. However, the 5 wt % DAC reinforced DAC/DSO composite exhibits the highest thermal stability, even higher than the pure ESO polymer matrix. The perfect dispersion and interaction between DAC and the DSO matrix may be the reason for it, which is consistent with the SEM analysis.

CONCLUSIONS

The ESO composites containing up to 25 wt % DAC and MCC were prepared by simple solution casting. Systematic comparisons were performed on microstructures, dynamic mechanical analysis, mechanical properties, and thermal stability of the composites. The results show that DAC leads to higher strength, modulus, and elongation at break than MCC does at the same filler loading. The 5 wt % DAC reinforced DAC/ESO composite shows the best toughness and the highest thermal stability due to the better dispersion and interfacial interaction. Tg of both MCC/ESO and DAC/ESO composites shift to a high temperature with the increase of the filler content, indicating that the cellulose fibers impart stiffness to the material. This study is important for proper selection of cellulose materials as reinforcing agents to the preparation of functional polymer composites.

ACKNOWLEDGMENTS

This work was supported by the Priority Academic Program Development of Jiangsu Higher Education and Natural Science Foundation of Jiangsu Province, China (BK 20141469). J.Y. acknowledges the support of Jiangsu Specially-Appointed Professor Program.

REFERENCES

1. Meier, M.; Metzger, J. O.; Schubert, U. S. *Chem. Soc. Rev.* **2007**, *36*, 1788.
2. Faruk, O.; Sain, M.; Farnood, R.; Pan, Y. F.; Xiao, H. N. *J. Polym. Environ.* **2014**, *22*, 279.
3. Keleş, E.; Hazer, B. *J. Polym. Environ.* **2009**, *17*, 153.
4. Petrović, Z. S.; Xu, Y.; Milić, J.; Glenn, G.; Klamczynski, A. *J. Polym. Environ.* **2010**, *18*, 94.
5. Çakmaklı, B.; Hazer, B.; Açıkgöz, Ş.; Can, M.; Cömert, F. B. *J. Appl. Polym. Sci.* **2007**, *105*, 3448.
6. Xia, Y.; Henna, P. H.; Larock, R. C. *Macromol. Mater. Eng.* **2009**, *294*, 590.
7. Andjelkovic, D. D.; Lu, Y.; Kessler, M. R.; Larock, R. C. *Macromol. Mater. Eng.* **2009**, *294*, 472.
8. Supanchaiyamat, N.; Shuttleworth, P. S.; Hunt, A. J.; Clark, J. H.; Matharu, A. S. *Green Chem.* **2012**, *14*, 1759.
9. Liu, Z.; Erhan, S. Z. *J. Am. Oil Chem. Soc.* **2010**, *87*, 437.
10. Zhang, J.; Hu, S.; Zhan, G. Z.; Tang, X. L.; Yu, Y. F. *Prog. Org. Coat.* **2013**, *76*, 1683.
11. Gerbase, A. E.; Petzhold, C. L.; Costa, A. P. O. *J. Am. Oil Chem. Soc.* **2002**, *79*, 797.
12. Kim, J. R.; Sharma, S. *Ind. Crop. Prod.* **2012**, *36*, 485.
13. Tan, S. G.; Ahmad, Z.; Chow, W. S. *Polym. Int.* **2014**, *63*, 273.

14. Supanchaiyamat, N.; Shuttleworth, P. S.; Hunt, A. J.; Clark, J. H.; Matharu, A. S. *Green Chem.* **2012**, *14*, 1759.
15. Tanrattanakul, V.; Saithai, P. *J. Appl. Polym. Sci.* **2009**, *114*, 3057.
16. Tsujimoto, T.; Uyama, H.; Kobayashi, S. *Polym. Degrad. Stabil.* **2010**, *95*, 1399.
17. Gupta, A. P.; Ahmad, S.; Dev, A. *Polym. Eng. Sci.* **2011**, *51*, 1087.
18. Jin, F.; Park, S. *Mater. Sci. Eng. A* **2008**, *478*, 402.
19. Altuna, F. I.; Espósito, L. H.; Ruseckaite, R. A.; Stefani, P. M. *J. Appl. Polym. Sci.* **2011**, *120*, 789.
20. Ratna, D. *Polym. Int.* **2001**, *50*, 179.
21. Tan, S. G.; Ahmad, Z.; Chow, W. S. *Polym. Int.* **2014**, *63*, 273.
22. Park, S.; Jin, F.; Lee, J. *Macromol. Rapid Commun.* **2004**, *25*, 724.
23. Cateto, C. A.; Barreiro, M. F.; Rodrigues, A. E.; Belgacem, M. N. *Ind. Eng. Chem. Res.* **2009**, *48*, 2583.
24. Ma, X. F.; Chang, P. R.; Yu, J. G. *Carbohyd. Polym.* **2008**, *72*, 369.
25. Luo, X.; Mohanty, A.; Misra, M. *Macromol. Mater. Eng.* **2013**, *298*, 412.
26. Sun, X.; Lu, C.; Liu, Y.; Zhang, W.; Zhang, X. *Carbohyd. Polym.* **2014**, *101*, 642.
27. Ashori, A.; Nourbakhsh, A. *Compos. B Eng.* **2010**, *41*, 578.
28. Kiziltas, A.; Gardner, D. J.; Han, Y.; Yang, H. *Thermochim. Acta* **2011**, *519*, 38.
29. Bai, W.; Li, K. *Compos. Part A: Appl. Sci. Manuf.* **2009**, *40*, 1597.
30. Li, H.; Wu, B.; Mu, C.; Lin, W. *Carbohyd. Polym.* **2011**, *84*, 881.
31. Lu, T. H.; Li, Q.; Chen, W. S.; Yu, H. P. *Compos. Sci. Technol.* **2014**, *94*, 132.
32. Sirviö, J.; Liimatainen, H.; Niinimäki, J.; Hormi, O. *Carbohyd. Polym.* **2011**, *86*, 260.
33. Xu, X. Z.; Liu, F.; Jiang, L.; Zhu, J. Y.; Haagenson, D.; Wiesenborn, D. P. *ACS Appl. Mater. Interfaces* **2013**, *5*, 2999.
34. Qiu, W. L.; Endo, T.; Hirotsu, T. *J. Appl. Polym. Sci.* **2004**, *94*, 1326.
35. Mathew, A. P.; Oksman, K.; Sain, M. *J. Appl. Polym. Sci.* **2005**, *97*, 2014.